INFLUENCE OF COLLECTIVITY ON REDUCED HINDRANCE FACTOR OF K-ISOMERS IN TANTALUM AND HAFNIUM ISOTOPES

Y.P. Singh, V. Kumar[†], A. Choudhary, A. Shukla
Manoj Kumar Sharma, P.K. Rath

Department of Physics, University of Lucknow-226007, India

Rohtash

Gurukul Kangri University, Haridwar-249404, India

P. Jain

Department of Physics, Sri Aurobindo College, University of Delhi-110017, India

Y. Kumar

Department of Physics, Deshbandhu College, University of Delhi-110019, India

R. Sapra

Department of Physics, Ramjas College, University of Delhi-110007, India

K. Jha

Dept. of Physics, Indian Inst. of Technology Ropar, Rupnagar-140001, India

M. Silarski, S. Sharma

Marian Smoluchowski Institute of Physics, Jagiellonian University
Łojasiewicza 11, 30-348 Kraków, Poland

Received 29 August 2022, accepted 2 February 2023,
published online 22 February 2023

The correlations of the reduced hindrance factor F_ν of the K-isomers in Ta and Hf isotopes with respect to N_pN_n (the product of valence nucleons), $E_K - E_R$ (the isomer excitation energy referred to a rigid rotor), and $E_K(N_n) - E_K(N_{n-\max})$ (the energy difference between the same configuration at N_n and $N_{n-\max}$ (middle of a shell), at given spin and isotopic chain) have been re-examined. The analysis is performed in the valence regions

[†] Corresponding author: vinod2.k2@gmail.com

divided into particle–particle (p–p), particle–hole (p–h), and hole–hole (h–h) regions, based on the N_pN_n phenomenology. The Ta and Hf isotopes are considered, given the availability of the same spin configuration in the different sectors of the valence regions. In our study, we observe that the parameter $E_K(N_n) - E_K(N_{n-\max})$ shows a significant correlation with F_ν, within an isotopic chain.

DOI:10.5506/APhysPolB.54.1-A4

1. Introduction

In nuclear spectroscopy, the lifetime of nuclear excited states is one of the most important observables which helps in developing the fundamental understanding of nuclear interaction and nuclear structure. Some of the excited states in nuclei may have a longer lifetime in comparison to other states, which indicates a peculiar nuclear structure [1–7]. These excited states, termed isomers, usually have a lifetime greater than the order of nanoseconds ($t_{1/2} \sim$ ns), and so far more than 2460 nuclear isomers with a half-life of 10 ns or more have been listed in the atlas of nuclear isomers [5]. The classification of these isomers [6, 7] is done based on nuclear structure details giving rise to the longer lifetime of excited nuclear states.

The lifetime τ of an excited nuclear state that decays by a single transition depends on the transition energy, E_γ, and the change in quantum numbers between the isomeric state and the state to which it decays, through the following relation [8]:

$$\tau \propto \frac{1}{(E_\gamma)^{2\lambda+1} \mid \langle f \mid T_\lambda \mid i \rangle \mid^2} \,,$$

where λ is the multipole order and T_λ is the transition operator between the initial, i, and final, f, states. The lifetime τ depends on three factors, *e.g.*, the gamma-transition energy, the multipole order, and the underlying transition matrix element. The latter is a model-dependent quantity and may vary significantly. If E_γ is small and the multipole order is large, the lifetime is likely to be relatively long, giving rise to an isomer state. Weisskopf estimated the electromagnetic transition rates due to the transition of a single nucleon from an initial state to a final state [9]; these estimates provide us with reasonable relative comparisons of the transition rates. The ratio of the experimental half-life $t_{1/2}^{\mathrm{Exp}}$ to the theoretical Weisskopf estimated half-life $t_{1/2}^{\mathrm{W}}$ of electromagnetic transition is known as the Weisskopf hindrance factor [7–10], F_{W}, and is given by

$$F_{\mathrm{W}} = \frac{t_{1/2}^{\mathrm{Exp}}(\text{Experimental})}{t_{1/2}^{\mathrm{W}}(\text{Weisskopf estimate})} \,.$$

When the experimental decay lifetime of γ-transition is several orders of magnitude higher than the Weisskopf estimate, it can be attributed to the poor matching of the initial and final wave functions, slowing down the transition rate. Similarly, if the transition rate is much higher than the Weisskopf estimate, more than one nucleon is expected to be responsible for the transition. The Weisskopf hindrance is used for the characterization of isomers.

In most of the deformed nuclei, the transition probabilities depend on the difference of the K quantum numbers of the initial and final states, denoted by ΔK [7, 11]. If this difference is larger than the multipole order λ of the electromagnetic transition, then such a transition is hindered by the degree of forbiddenness (also known as K-forbiddenness) given by $\nu = \Delta K - \lambda$. The degree of K-forbiddenness, ν, can be further used to define the reduced-hindrance factor F_ν [12–14], expressed as

$$F_\nu = (F_{\mathrm{W}})^{1/\nu} . \qquad (1)$$

For example, for the $J^\pi = 8^-$ isomer in ^{180}Hf (located at $E_x = 1141$ keV, with $t_{1/2} = 5.47$ h), $F_{\mathrm{W}} = 2.86 \times 10^{16}$ and $F_v = 224$ [15]. The reduced-hindrance factor also depends on K mixing in both initial and final states [15], and leads to a low hindrance factor. The K mixing arises due to the Coriolis effect, which intensifies with decreasing neutron and proton numbers in the lower half of the shells due to the population of high-j, low-Ω orbitals. In contrast, greater axial asymmetry occurs with increasing neutron and proton numbers in the upper half of the shells, leading to an increase in K mixing associated with γ tunneling, where γ is the axial asymmetry parameter.

The systematic effect of Coriolis and γ-induced K mixing may be well characterized through a single variable, N_pN_n. The N_pN_n [16–19] is the product of the number of valence protons (N_p) and neutrons (N_n), relative to the nearest closed shells (counted as a number of holes past the mid shell). For example, the N_p and N_n values are counted as follows: for $^{118}_{56}$Ba$_{62}$, $N_p = 6$, $N_n = 12$; for $^{128}_{56}$Ba$_{72}$, $N_p = 6$, $N_n = 10$; for $^{154}_{70}$Yb$_{84}$, $N_p = 12$, $N_n = 2$, and for $^{172}_{70}$Yb$_{102}$, $N_p = 12$, $N_n = 20$. The N_pN_n reflects the characteristics of the deformation. The deformation increases with N_pN_n. Here, one would expect a correlation with hindrance factors since low values of N_pN_n (*i.e.* small deformation) imply higher rotational frequencies (for a given spin) and large Coriolis effects, resulting in more K mixing in both initial and final states. The K mixing increases with increasing level density [20] and level density appears as dependence on the isomer's excitation energy relative to a rigid rotor ($E_K - E_R$). Furthermore, strong correlations have been observed between the reduced-hindrance factor and other variables [15, 21], namely, the isomer energy relative to a rigid rotor [22] and the quasi-particle configurations involved [23].

The correlation of F_ν with N_pN_n needs to be re-examined as some of the earlier studies [24–26] showed a good correlation (see Fig. 1 (a) as an example), whereas other work [27] showed almost no correlation (see Fig. 1 (b)). The graph shows data from Refs. [26, 27]. In the present work, we re-examined the correlation of F_ν with N_pN_n, $E_K - E_R$, and $E_K(N_n) - E_K(N_{n-\max})$ for different valence regions based on the particle and the hole consideration. The $E_{N_pN_n} - E_{(N_pN_n)_{\max}}$ is the isomer energy relative to the isomer at $N_{n-\max}$. An isotopic chain can be divided into particle–particle (p–p), hole–hole (h–h), and particle–hole (p–h) valence regions [17, 18, 28]. This means that both the proton and neutron are in the first half of the shell (p–p), or both in the second half (h–h), and one fills below and the other above the mid shell (p–h) The tantalum and hafnium isotope series were preferred due to the availability of the same spin configuration isomer data in (h–p) and (h–h) valence regions, in spite of unavailability of data in the p–p region for these series. For the sake of consistency, the F_ν values from the E1, E2, and M1 decay branches have been preferred in the present study.

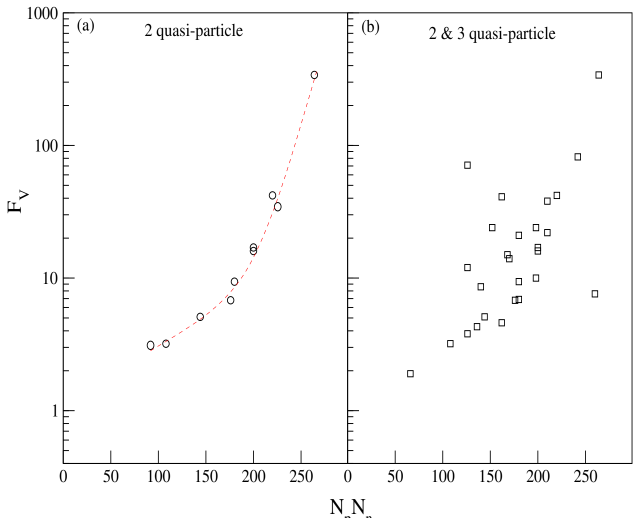

Fig. 1. The reduced hindrance of E2, $\nu \geq 4$ transitions for (a) two quasi-particle isomer data [26] and (b) two- and three-quasi-particle isomers data [27] in the $N = 82$–126 shell as a function of N_pN_n. The fit-dashed line is of the form of $F_\nu = A + \exp[(N_pN_n - 80)^B/C]$ [26, 27], where $A = 2.3$, $B = 1.873$, and $C = 3\times10^3$.

2. *K*-isomer

The shell model [29] predicts the existence of isomers when excited states require large multipole order or/and low-energy γ-transitions for their decay. Nuclei with or/near the magic number (Z, $N = 2$, 8, 20, 28, 50, 82, 126) are more or less spherical in their ground state, and as one moves towards the mid shell, the nuclear shape usually becomes deformed. An example of a prolate shape, with symmetry about the long axis, is shown in Fig. 2 (a) and 2 (b). The deformed-shell model (Nilsson model [30, 31]) predicts the existence of isomers in non-spherical nuclei [12–14]. A deformed even–even nucleus rotates around an axis perpendicular to the axis of symmetry, resulting in the ground-state band populated with $I^\pi = 0^+$ and $K = 0$ (see Fig. 2 (a)). Excitation of the nucleus can break up a pair of nucleons and move one or both nucleons to higher orbits. This excitation is called a two quasi-particle [7] state, emphasizing the importance of the pairing interaction [31, 35], which changes the energy and wave function of the nuclear level. When a pair of nucleons breaks near the Fermi surface, the quasi-particle spins (j_1, j_2) can be aligned along the symmetry axis, leading to a high K-value $(\sum \Omega_i = K)$, where $\Omega_i = 1, 2$ is the projection of the single-particle angular momentum $j_i = 1, 2$. With such an orientation as shown in Fig. 2 (b), the spin of the band-head results from completely unpaired nucleons rather than collective rotation. Other excited states of the band can arise either from unpaired nucleons or from the rotation of the core. For example, the 4^+ state in Fig. 2 (b) is a K-isomer, where the $\nu(= 3, 2)$, where $\Delta K = 4$ and $\lambda = 1, 2$.

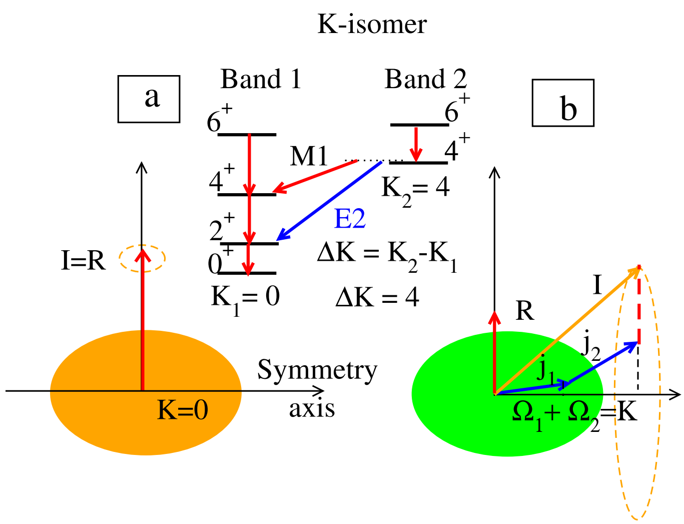

Fig. 2. (a) Schematic diagrams showing a collective rotation band (Band 1) with $I^\pi = 0^+$, $K = 0$ of an even–even nucleus. (b) A collective rotation band (Band 2), with $I^\pi = 4^+$, $K = 4$, and the coupling scheme of two individual nucleons (after breaking pair) with the collective rotation of the core.

3. F_ν systematics with N_pN_n, $E_K - E_R$, and $E_K(N_n) - E_K(N_{n-\max})$

3.1. F_ν correlation with N_pN_n in different valence regions

The collectivity grows faster in the p–p and h–h valence regions compared to the p–h/h–p valence region [28]. To check the effect on F_ν values, the data have to be shown for (p–p), (h–p), and (h–h) valence regions separately. In the present study, for the above purpose, the tantalum ($J^\pi = 21/2^-$) and hafnium ($J^\pi = 6^+, 8^-$) isotopes for which the same spin configuration isomers data are available for p–h and h–h regions have been considered and listed in Table 1. The F_ν values were calculated with respect to decaying branches via M1, E1, and E2 multipolarities.

Figure 3 shows the comparison of $\log F_\nu$ values with N_pN_n in split valence regions and non-split valence regions based on particle–hole consideration. Clearly, the $\log F_\nu$ values in Fig. 3 (a), and (e) appear to be scattered. However, Fig. 3 (b), (d), and (f) shows interesting trends by seeing the same data plotting in hole–hole (h–h) and hole–particle (h–p) regions. Remarkably, the $\log F_\nu$ values are increasing with decreasing state excitation energy in different valence regions, which has not been discussed before. The $\log F_\nu$ value of ^{179}Ta is showing anomalous behavior which can be interpreted in terms of strong configuration mixing [15, 36, 37].

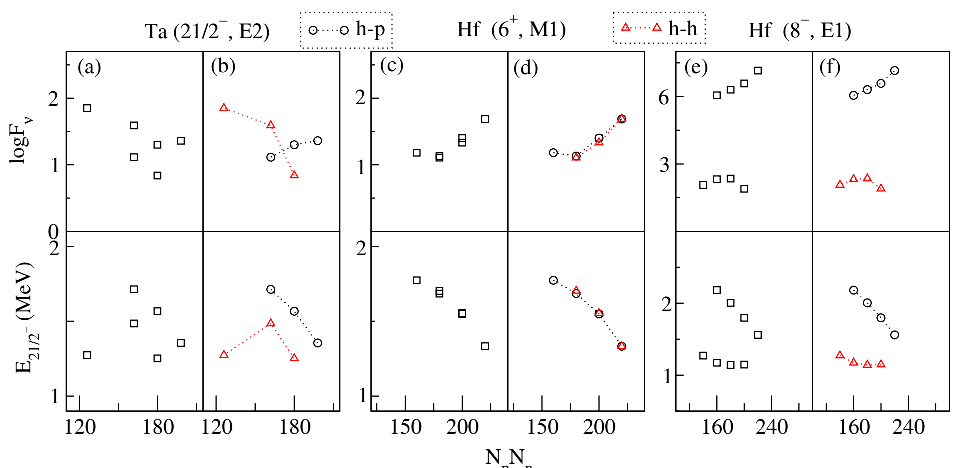

Fig. 3. The upper panels show $\log F_\nu$ values and the lower panels show exited states energy, plotted against N_pN_n for tantalum and hafnium isotopes. Data in (b), (d), (f) panels are shown divided into hole–hole (h–h) and hole–particle (h–p) valence regions. Data in (a), (c), (e) panels are shown without particle–hole distinction. The dotted lines are drawn for visual aid.

Table 1. The F_{W} and F_{ν} values listed for the branch decaying via M1, E1, and E2 multipolarities and configurations of the isomeric states, according to the Nilsson model (from Refs. [15, 27, 32–34, 36–38]).

Nuclide	Valence region	$N_p N_n$	$J^{\pi} \equiv K$	$\sigma\lambda$	$t_{1/2}^{\mathrm{Exp}}$	F_{W}	F_{ν}	$\log F_{\mathrm{W}}$	$\log F_{\nu}$	Neutron configuration	Proton configuration
^{170}Hf	h–p	160	6^+	M1	$\leq$5.0 ns	$\leq$8.2E+5	$\leq$15.20	$\leq$5.91	$\leq$ 1.18		$5/2^+$[402], $7/2^+$[404]
			8^-	E1	23(2) ns	1.13(10)E+6	1.13(10)E+6	6.05	6.05		$7/2^+$[404], $9/2^-$[514]
^{172}Hf	h–p	180	6^+	M1	4.8(4) ns	4.6(4)E+5	13.55(24)	5.65	1.13		$5/2^+$[402], $7/2^+$[404]
			8^-	E1	163(3) ns	2.03(5)E+6	2.03(5)E+6	6.30	6.30		$7/2^+$[404], $9/2^-$[514]
^{174}Hf	h–p	200	6^+	M1	138(4) ns	9.6(3)E+6	24.89(16)	6.98	1.39		$5/2^+$[402], $7/2^+$[404]
			8^-	E1	2.39(4) μs	3.46(9)E+6	3.46(9)E+6	6.54	6.54	$7/2^-$[514], $9/2^+$[624]	
^{176}Hf	h–p/h–h	220	6^+	M1	9.5(2) μs	2.75(12)E+8	48.8(4)	8.43	1.68	61% $5/2^-$[512], $7/2^-$[514]	39% $5/2^+$[402], $7/2^+$[404]
			8^-	E1	9.8(2) μs	1.44(7)E+7	1.44(7)E+7	7.15	7.15	38% $7/2^-$[514], $9/2^+$[624]	62% $7/2^+$[404], $9/2^-$[514]
^{178}Hf	h–h	200	6^+	M1	77.5(7) ns	4.65(11)E+6	21.55(10)	6.66	1.33		$5/2^+$[402], $7/2^+$[404]
			8^-	E1	4.0(2) s	1.95(10)E+13	79.2(6)	13.29	1.89	64% $7/2^-$[514], $9/2^+$[624]	36% $7/2^+$[404], $9/2^-$[514]
^{180}Hf	h–h	180	6^+	M1	2.8(3) ns	3.5(4)E+5	12.8(3)	5.54	1.10		$5/2^+$[402], $7/2^+$[404]
			8^-	E1	5.47(4) h	2.86(25)E+16	224.4(3)	16.45	2.35		$7/2^+$[404], $9/2^-$[514]
^{182}Hf	h–h	160	8^-	E1	61.5(15) m	1.73(17)E+16	209(3)	16.23	2.32		$7/2^+$[404], $9/2^-$[514]
^{184}Hf	h–h	140	8^-	E1	48.0(10) s	2.9(7)E+14	116(4)	14.46	2.06		$7/2^+$[404], $9/2^-$[514]
^{173}Ta	h–p	162	$21/2^-$	E2	148(4) ns	2.3 (4)E+4	12.3(6)	4.36	1.11		$5/2^+$[402], $7/2^+$[404], $9/2^-$[514]
^{175}Ta	h–p	180	$21/2^-$	E2	1.95(15) μs	1.8(3)E+5	20.6(8)	5.25	1.30		$5/2^+$[402], $7/2^+$[404], $9/2^-$[514]
^{177}Ta	h–p/h–h	198	$21/2^-$	E2	5.31(25) μs	2.8(3)E+5	23.0(7)	5.44	1.36		$5/2^+$[402], $7/2^+$[404], $9/2^-$[514]
^{179}Ta	h–h	180	$21/2^-$	E2	322(16) ns	2.22(20)E+3	6.87(16)	3.53	0.83		$5/2^+$[402], $7/2^+$[404], $9/2^-$[514]
^{181}Ta	h–h	162	$21/2^-$	E2	25(2) μs	2.3(4)E+6	39.0(17)	6.36	1.59		$5/2^+$[402], $7/2^+$[404], $9/2^-$[514]
^{185}Ta	h–h	126	$21/2^-$	E2	11.8(14) ms	2.5(4)E+7	71(3)	7.39	1.85	$3/2^-$[512], $11/2^+$[615]	$7/2^+$[404]

3.2. F_ν correlation with $E_K - E_R$ and $E_K(N_n) - E_K(N_{n-\max})$ for different valence regions

Figure 4 shows $\log F_\nu$ as a function of isomer energy relative to a rigid rotor, $E_K - E_R$. The rotor energy, $E_R = \frac{\hbar^2}{2\mathcal{J}} I(I+1)$ with $I \equiv K$, which is considered from [20, 27, 36]. The $\log F_\nu$ values are expected to be correlated with the $E_K - E_R$.

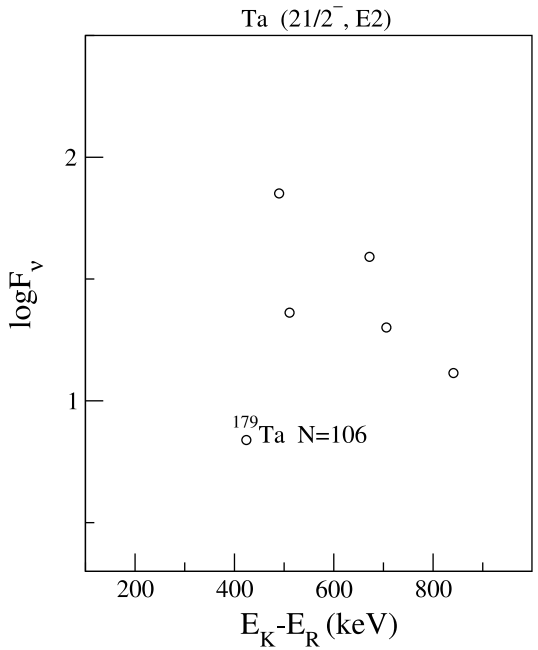

Fig. 4. The reduced hindrance factors as a function of isomer energy relative to a rigid rotor, $E_K - E_R$.

Figure 5 shows $\log F_\nu$ as a function of isomer energy relative to a rigid rotor, $E_K - E_R$ and $E_K(N_n) - E_K(N_{n-\max})$ for different valence regions for the states of tantalum and hafnium isotopes with spin and parity $J^\pi = 21/2^-$ and 6^+, 8^-, respectively. Similar trends are observed in different valence regions with $E_K(N_n) - E_K(N_{n-\max})$ (see Fig. 5). This correlation can be described by a polynomial of degree 2 (see Fig. 6). However, there is no similar trend observed for tantalum isotopes when plotted with respect to $N_p N_n$ for different valence regions (see Fig. 3 (b)). The $\log F_\nu$ value of ^{179}Ta is showing anomalous behavior as observed from the overall data trend, which can be interpreted in terms of strong configuration mixing [15, 36, 37].

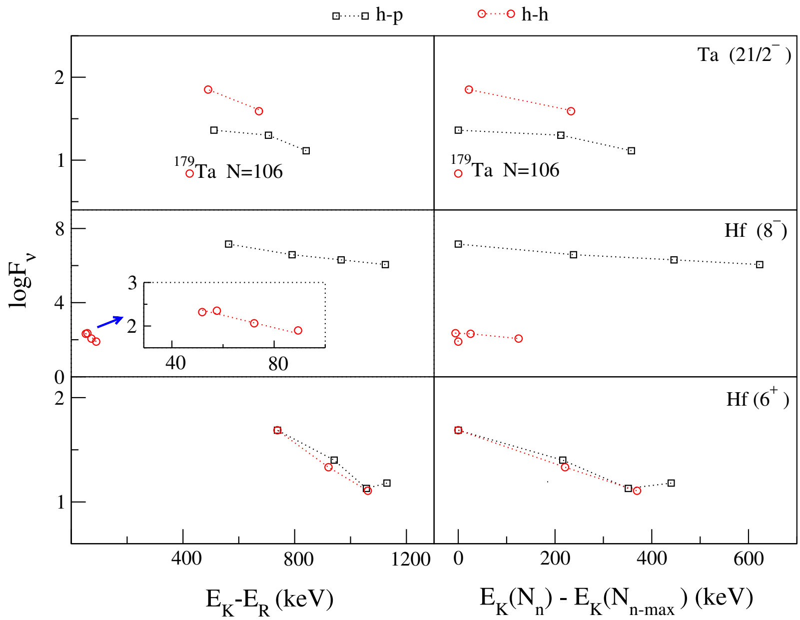

Fig. 5. Figure shows $\log F_\nu$ as a function of isomer energy relative to a rigid rotor, $E_K - E_R$ and $E_K(N_n) - E_K(N_{n-\max})$ for different valence regions. The dotted lines are drawn for visual aid.

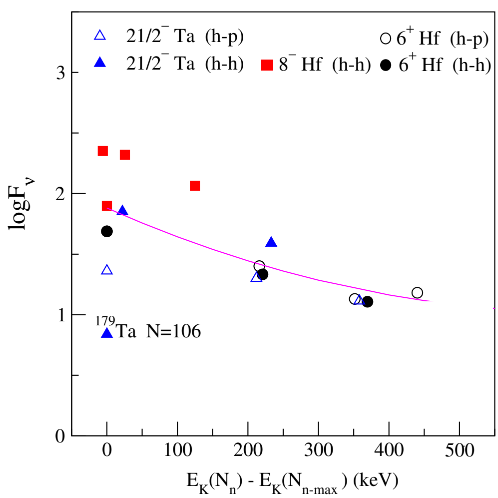

Fig. 6. The $\log F_\nu$ values as a function of $E_K(N_n) - E_K(N_{n-\max})$ are shown separately and as a whole in the regions h–p and h–h. The solid line is defined by the equation $\log F_\nu = a\,\xi^2 + b\,\xi + c$, where $\xi = E_K(N_n) - E_K(N_{n-\max})$. The parameters are $a = 1.91818e-06$, $b = -0.00256$, and $c = 1.88045$.

4. Conclusion

The correlation of reduced-hindrance factor F_ν with N_pN_n has been re-examined for the K-isomers of tantalum and hafnium isotopes. Earlier studies related to the correlation showed a good correlation for two quasi-particles and almost no correlation for two- and three-quasi-particle isomers. In the present work, we have found that this contradiction weakens when the correlation is viewed in the valence regions divided into particle–particle, particle–hole, and hole–hole regions based on N_pN_n phenomenology. The $\log F_\nu$ values seem to increase with decreasing state excitation energy in different valence regions. The known correlation of F_ν with the isomer energy relative to a rigid rotor, $E_K - E_R$, is more clearly observed in different valence regions. A new correlation of F_ν with the isomer energy relative to the middle shell isotope isomer, $E_K(N_n) - E_K(N_{n-\max})$, has been proposed which can be described by a polynomial of degree 2. However, a quantitative understanding of these correlations remains elusive. Expansion of these ideas along with the availability of more experimental data will provide a better understanding of the decay rates from isomers in deformed regions which could be quite promising for nuclear structure studies.

Financial assistance from the University Grant Commission (UGC) and Inter University Accelerator Centre (IUAC), New Delhi is gratefully acknowledged.

REFERENCES

[1] F. Soddy, «The Stability of Lead Isotopes from Thorium», *Nature* **99**, 244 (1917).

[2] F. Soddy, «The Complexity of the Chemical Elements II», *Nature* **99**, 433 (1917).

[3] O. Hahn, «Über eine neue radioaktive Substanz im Uran», *Chem. Berichte* **54**, 1131 (1921).

[4] C.F. von Weizsäcker, «Metastabile Zustände der Atomkerne», *Naturewissenschaften* **24**, 813 (1936).

[5] A.K. Jain *et al.*, «Atlas of Nuclear Isomers», *Nucl. Data Sheets* **128**, 1 (2015).

[6] A.K. Jain, B. Maheshwari, A. Goel, «Nuclear Isomers: A Primer», *Springer International Publishing*, Cham 2021.

[7] P.M. Walker, G.D. Dracoulis, «Energy traps in atomic nuclei», *Nature* **399**, 35 (1999).

[8] G.D. Dracoulis, «Isomers, nuclear structure and spectroscopy», *Phys. Scr.* **T152**, 014015 (2013).

[9] J.M. Blatt, V.F. Weisskopf, «Theoretical Nuclear Physics», *John Wiley & Sons Inc.*, New York, London 1952.

[10] P.M. Walker, F.R. Xu, «High-K isomerism in rotational nuclei», *Phys. Scr.* **91**, 013010 (2016).

[11] G. Alaga, K. Alder, A. Bohr, B.R. Mottelson, «Intensity rules for beta and gamma transitions to nuclear rotational states», *Dan. Vid. Sel. Mat. -fys. Medd.* **29**, 9 (1955).

[12] C.J. Gallagher, «Classification of beta- and gamma-ray transitions between intrinsic states in deformed even-mass nuclei», *Nucl. Phys.* **16**, 215 (1960).

[13] K.E.G. Löbner, «Systematics of absolute transition probabilities of K-Forbidden gamma-ray transitions», *Phys. Lett. B* **26**, 369 (1968).

[14] L.I. Rusinov, «Nuclear Isomerism», *Sov. Phy. Usp.* **4**, 282 (1961).

[15] F.G. Kondev, G.D. Dracoulis, T. Kibédi, «Configurations and hindered decays of K isomers in deformed nuclei with $A > 100$», *At. Data Nucl. Data Tables* **103–104**, 50 (2015).

[16] R.F. Casten, «A simple approach to nuclear transition regions», *Phys. Lett. B* **152**, 145 (1985).

[17] R.F. Casten, «Possible Unified Interpretation of Heavy Nuclei», *Phys. Rev. Lett.* **54**, 1991 (1985).

[18] R.F. Casten, N.V. Zamfir, «Valence correlation schemes and signatures of nuclear structure: A simple global phenomenology for $B(E2 : 2_1^+ \to 0_1^+)$ values», *Phys. Rev. Lett.* **70**, 402 (1993).

[19] V. Kumar, S. Kumar, G. Gangopadhyay, D. Negi, «Correlation between ground state lifetime and valence nucleons for isotopic chains», *Mod. Phys. Lett. A* **29**, 1450102 (2014).

[20] P.M. Walker *et al.*, «K-forbidden transitions from multi-quasiparticle states», *Phys. Lett. B* **408**, 42 (1997).

[21] T.P.D. Swan *et al.*, «Discovery of isomers in dysprosium, holmium, and erbium isotopes with $N = 94$ to 97», *Phys. Rev. C* **85**, 024313 (2012).

[22] Y. Liu *et al.*, «Systematic study of spin assignments and signature inversion of $\pi h_{11/2} \otimes \nu h_{11/2}$ bands in doubly odd nuclei around $A \sim 130$», *Phys. Rev. C* **54**, 719 (1996).

[23] G.D. Dracoulis, F.G. Kondev, P.M. Walker, «Pairing reduction and rotational motion in multi-quasiparticle states», *Phys. Lett. B* **419**, 7 (1998).

[24] P.M. Walker, «High-K isomers: some of the questions», *EPJ Web Conf.* **123**, 01001 (2016).

[25] P.M. Walker, «Isomer building blocks and K-forbidden decays», *Phys. Scr.* **92**, 054001 (2017).

[26] T.P.D. Swan *et al.*, «Discovery of a nonyrast $K^\pi = 8^+$ isomer in ^{162}Dy, and the influence of competing K-mixing mechanisms on its highly forbidden decay», *Phys. Rev. C* **83**, 034322 (2011).

[27] P.M. Walker, S. Lalkovski, P.D. Stevenson, «Configuration dependence of K-forbidden transition rates from three-quasiparticle isomers», *Phys. Rev. C* **81**, 041304(R) (2010).

[28] R.B. Cakirli, R.F. Casten, «Direct Empirical Correlation between Proton–Neutron Interaction Strengths and the Growth of Collectivity in Nuclei», *Phys. Rev. Lett.* **96**, 132501 (2006).

[29] M.G. Mayer, «On Closed Shells in Nuclei. II», *Phys. Rev.* **75**, 1969 (1949).

[30] S.G. Nilsson, «Binding States of Individual Nucleons in Strongly Deformed Nuclei», *Dan. Vid. Sel. Mat. -fys. Medd.* **29**, 16 (1955).

[31] I. Ragnarsson, S.G. Nilsson, «Shapes and Shells in Nuclear Structure», *Cambridge University Press*, 1995.

[32] R.T. Wood *et al.*, «Three-quasiparticle isomer in ^{173}Ta and the excitation energy dependence of K-forbidden transition rates», *Phys. Rev. C* **95**, 054308 (2017).

[33] F.G. Kondev *et al.*, «Intrinsic states and rotational bands in ^{175}Ta», *Nucl. Phys. A* **601**, 195 (1996).

[34] M. Dasgupta *et al.*, «Competition between high-K states and rotational structures in ^{177}Ta», *Phys. Rev. C* **61**, 044321 (2000).

[35] P. Ring, P. Schuck, «The Nuclear Many-Body Problem», *Springer Berlin Heidelberg*, Berlin, Heidelberg 1980.

[36] P.M. Walker, P.D. Stevenson, «Configuration mixing and K-forbidden E2 decays», *Phys. Rev. C* **103**, 064305 (2021).

[37] F.G. Kondev *et al.*, «Multi-quasiparticle states in ^{179}Ta and structural changes in the yrast line of the odd tantalum isotopes», *Nucl. Phys. A* **617**, 91 (1997).

[38] C. Wheldon *et al.*, «Opening up the $A \sim 180$ K-isomer landscape: inelastic excitation of new multi-quasiparticle yrast traps», *Phys. Lett. B* **425**, 239 (1998).